World Academy of Science, Engineering and Technology
International Journal of Chemical and Materials Engineering
Vol:11, No:1, 2017

# Electrochemical Performance of Al-$Mn_2O_3$ Based Electrode Materials

Noor Ul Ain Bhatti, M. Junaid Khan, Javed Ahmad, Murtaza Saleem, Shahid M. Ramay, Saadat A. Siddiqi



***Abstract*****—**Manganese oxide is being recently used as electrode material for rechargeable batteries. In this study, Al incorporated $Mn_2O_3$ compositions were synthesized to study the effect of Al doping on electrochemical performance of host material. Structural studies were carried out using X-ray diffraction analysis to confirm the phase stability and explore the lattice parameters, crystallite size, lattice strain, density and cell volume. Morphology and composition were analyzed using field emission scanning electron microscope and energy dispersive X-ray spectroscopy, respectively. Dynamic light scattering analysis was performed to observe the average particle size of the compositions. FTIR measurements exhibit the O-Al-O and O-Mn-O and Al-O bonding and with increasing the concentration of Al, the vibrational peaks of Mn-O become sharper. An enhanced electrochemical performance was observed in compositions with higher Al content.

***Keywords*****—**$Mn_2O_3$, electrode materials, energy storage and conversion, electrochemical performance.

## I. Introduction

THE tailoring of layered oxide materials have been widely discussed subject as a source for portable energy storage devices. Numerous materials have been proposed that proved to be a good candidate for advanced technologies including batteries, fuel cells, solar cells and super capacitors [1], [2]. The advancement in search of energy storage materials enforce us to make cost efficient and maximum storage capacity materials which could be used for portable electronic devices and hybrid electronic vehicles. In recent electronic applications, lithium ion batteries are preferably used as they have high coulombic energy efficiency, magnificent low self-discharge rate and lack of memory effect [3], [4]. Graphite is enormously used as commercial material for lithium ion batteries but due to its low storage capacity, energy, power density, longer life cycle and improved safety there is a need to search new materials as layered oxides as a use for better electrode material [5]. To enhance storage capacity of Li ion batteries, transition metal oxides in nano-structured materials have been extensively studied [6], [7]. Among all transition metal oxides [8] such as manganese oxide [9], [10], ruthenium oxide [11], cobalt oxide [12], [13], nickel oxide [14], copper oxide [15], manganese oxide is considered as the most reliable electrode material because of their abundance, non-toxicity, low cost, multiple high theoretical capacitance and environmental compatibility. Ruthenium oxide is toxic and other materials have also limited in their use so we prefer manganese oxide [16], [17]. A number of research studies have been done on synthesis of nanostructured manganese oxide with different experimental techniques such as physical vapor deposition, chemical bath deposition, sputtering [18] and sol-gel methods [19]. Elemental doping of simple metal oxides to form mixed metal oxides has been a way to boost up their electrochemical activities, electronic conductivity and to minimize their cost efficiency. In this case, binary systems doping is preferable such as NiMn, MnCo [20], MnFe [21], NiCo [22], SnAl oxides and ternary metal oxides systems like Mn-Ni-Co [23], [24], Co-Ni-Cu [25] and Mn-Ni-Cu oxides [26]. In present research work, we study sol-gel synthesized nanostructured $Mn_2O_3$ with doping combination of Al. The samples are physically characterized by X-Ray diffraction (XRD), field emission scanning electron microscope (FESEM), energy dispersive X-ray spectroscopy (EDS), dynamic light scattering, Fourier transform infrared spectroscopy (FTIR), and electrochemical measurements. The effect of Al substitution on all these properties of $Mn_2O_3$ was precisely studied and found that electrochemical performance was significantly enhanced.

Noor Ul Ain Bhatti, M. Junaid Khan, and Javed Ahmad are with the Laboratory of Experimental and Theoretical Physics, Department of Physics, Bahauddin Zakariya University (60800), Multan, Pakistan.

Murtaza Saleem is with the Department of Physics, Syed Babar Ali School of Sciences and Engineering (SBASSE), Lahore University of Management Sciences (LUMS), Opposite Sector U, DHA, Lahore 54792, Pakistan.

Shahid M. Ramay is with the College of Science, Department of Physics and Astronomy, King Saud University, Riyadh, Saudi Arabia.

Saadat A. Siddiqi is with the Interdisciplinary Research Centre in Biomedical Materials, COMSATS Institute of Information Technology, M.A. Jinnah Campus, Lahore-54600, Pakistan (Corresponding Author; phone: +92-300-4866616; e-mail: saadat.anwar@ciitlahore.edu.pk).

## II. Experimental Section

### A. Synthesis

Al doped $Mn_2O_3$ nanostructured compositions were synthesized using well established sol-gel based fuel agent assisted self-combustion technique. Stoichiometric molar ratios of analytical research grade aluminium nitrate [$Al(NO_3)_2.9H_2O$] and manganese nitrate [$Mn(NO_3)_2.4H_2O$] were use as the sources of Al and Mn, respectively. In this preparation, glycine was used as the fuel agent. Calculated molar amounts of reagents for undoped and Al doped $Mn_2O_3$ were weighed on a precise digital balance and subsequently dissolved in 25 ml distilled water. The solution was kept on hot place at 250 °C with constant stirring inside a clean fume hood environment. The temperature of the attained gel was raised to 350 °C and stirring was subsequently stopped. Fine powder of brownish black color was obtained after intense exothermic combustion reaction. The resulting products were dried and calcinated at 600 °C for 4 hours, subsequently, a

dark brownish powder was obtained for each composition. The powder was grinded well using mortar and pestle until fine, homogenous and uniform sized particles were achieved.

*B. Characterizations*

Structural studies were carried out using XRD instrument (Bruker D-2 Phaser) operating at 30 kV and 10 mA using Cu K-alpha radiation (λ=1.5406 Å) and a step scan size of 0.05°. A FESEM (FEI Nova 450) was used to observe the morphology of the samples. Qualitative and quantitative elemental compositions were confirmed using EDS spectrometry (Oxford Instrument Inca X-Act). FTIR analysis were carried out using Bruker Alpha instrument. Chinstruments 660E was used to extract the first charge-discharge curves and cyclic performance of all the synthesized compositions.

## III. Results and Discussion

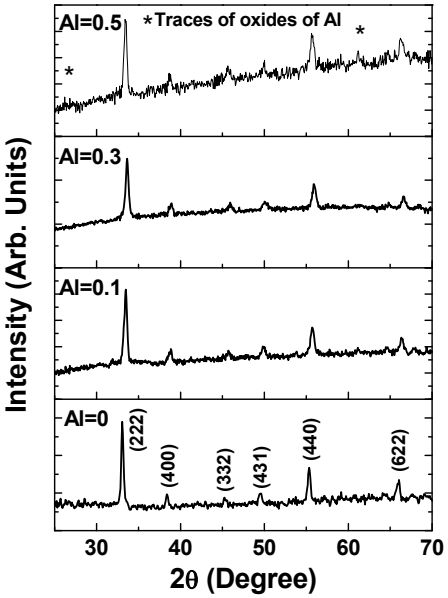


Fig. 1 XRD spectra of undoped and Al doped compositions

The XRD spectra of undoped and Al doped $Mn_2O_3$ are shown in Fig. 1. All the peaks in XRD patterns are exactly matched with the host $Mn_2O_3$ standard pattern containing JCPD card number 76-0150. However, some traces of oxides of Al were observed and clearly appeared in composition with highest content of Al and this showing some different behavior as compared to other spectra. It is clear that there are visible peak shifts to higher angle in the spectrum which is consistent to the previously reported substitutions [27], [28] with lower ionic radii. Crystallite size, cell volume, lattice constant and lattice strain were calculated and observed a significant variation in it with doping of Al content. Crystallite size and cell volume was observed as 43-53 nm and 784-824 $Å^3$, respectively as shown in Table I. A significant variation in lattice constant (9.22-9.38 Å) and lattice strain (2.64-15.57) was also observed revealed the doping of Al content in to $Mn_2O_3$ structure.

The microstructural studies were carried out using FESEM equipped with EDX detector. Fig. 2 presents the FESEM micrographs of undoped and Al doped $Mn_2O_3$ samples. It is visible through images that morphologies are oriented in non-uniform arrangement but they have distinct boundaries and clear shapes like microspheres and fillets with some compact shapes, as well as few cavities in them. Particles are present in random sizes which are estimated as 94.57 nm for $Al_{0.1}Mn_{1.9}O_3$, 144 nm for $Al_{0.3}Mn_{1.7}O_3$ and 172 nm for $Al_{0.5}Mn_{1.5}O_3$ samples. The particles in Al doped $Mn_2O_3$ are observed to be arranged more densely because of relatively smaller size of Al.

Fig. 3 represents the EDX spectra for all of the four samples. The EDX analysis reveals that Mn, O and Al contents are present in the approximate stoichiometric ratios in the samples, which ensure the incorporation of Al constituents in the host $MnO_2$ structure. Traces of very small carbon content might visible just because of the sample remnant. Quantitative EDX analysis is approximately according to the dissolved molar ratio for added elements in all samples as given in Table II.

FITR spectra of $Mn_2O_3$ and doped with different concentrations of Al are studied in the range 400-550 $cm^{-1}$ as shown in Fig. 4 (a) which reveals the presence of O-Mn-O and O-Al-O stretching modes. The transmittance spectra of undoped and doped samples have considerable differences among them. Most of the transmission bands are stretched between the wavelength 400-550 $cm^{-1}$. The wide band appearing from 500 $cm^{-1}$ onward correspond to vibrational frequencies of coordinate O-Al-O bond [29]. Low frequency band in the viscinity of 419 $cm^{-1}$ correspond to the change in O-Mn-O bond angle [30]. Other bonds in the range 400-500 $cm^{-1}$ is correspond to the Al-O vibrations [31]. As we increase Al concentration, we observe that Mn-O vibrational peak at ~ 500 $cm^{-1}$ appear to be sharper.

TABLE I
Lattice Constant, Crystallite Size, Cell Volume, Lattice Strain and Density of Compositions

| Sample | Lattice Constants (Å) | Crystallite Size (nm) | Cell Volume ($Å^3$) | Lattice strain($\times 10^{-3}$) | Density ($gcm^{-1}$) |
|---|---|---|---|---|---|
| **Undoped** | 9.38 | 44 | 824.50 | 2.64 | 5.08 |
| **$Al_{0.1}Mn_{1.9}O_3$** | 9.27 | 53 | 795.82 | 12.04 | 6.17 |
| **$Al_{0.3}Mn_{1.7}O_3$** | 9.22 | 53 | 784.7 | 15.57 | 6.26 |
| **$Al_{0.5}Mn_{1.5}O_3$** | 9.27 | 45 | 796.3 | 11.75 | 6.17 |

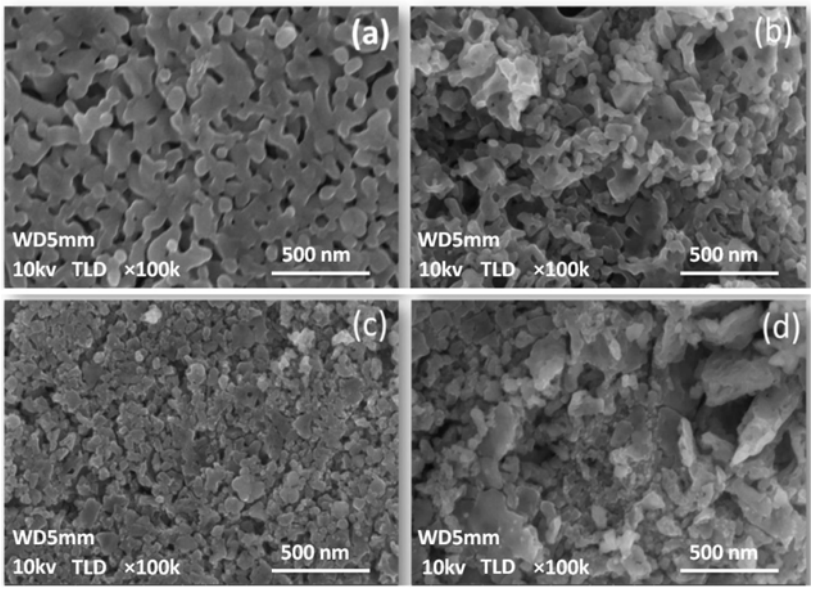


Fig. 2 FESEM micrographs of undoped and Al doped compositions

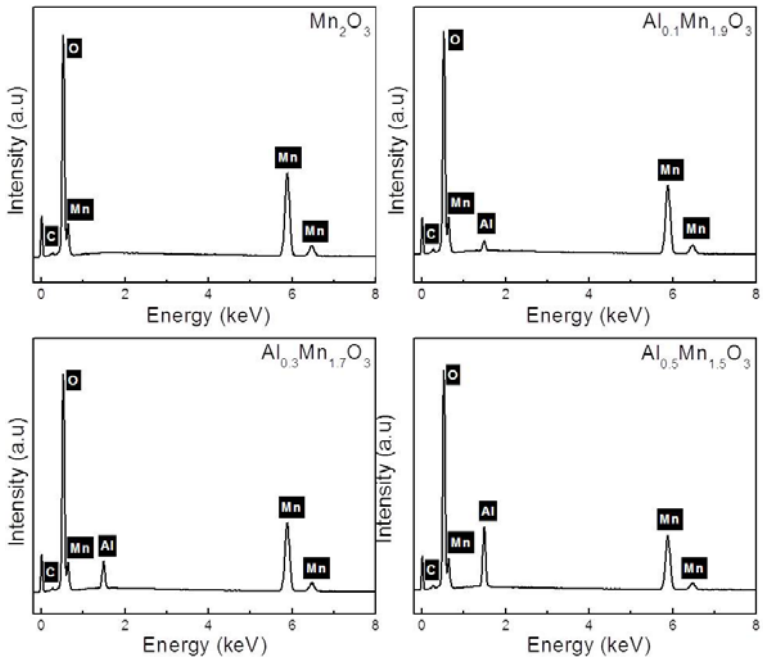


Fig. 3 EDX spectra of undoped and Al doped compositions

TABLE II
EDX ELEMENTAL COMPOSITIONAL MEASUREMENTS

| | Undoped | | $Al_{0.1}Mn_{1.9}O_3$ | | $Al_{0.3}Mn_{1.7}O_3$ | | $Al_{0.5}Mn_{1.5}O_3$ | |
|---|---|---|---|---|---|---|---|---|
| | At.% | Wt.% | At. % | Wt.% | At. % | Wt.% | At.% | Wt.% |
| **O** | 62.27 | 34.08 | 64.15 | 37.53 | 63.56 | 37 | 64.28 | 40.69 |
| **Al** | 0 | 0 | 1.69 | 1.66 | 4.32 | 4.24 | 8.78 | 9.38 |
| **Mn** | 34.34 | 64.53 | 29.17 | 58.61 | 28.64 | 57.24 | 21.86 | 47.52 |
| **C** | 3.39 | 1.39 | 4.99 | 2.2 | 3.48 | 1.51 | 5.08 | 2.41 |
| **Total** | | | | **100** | | | | |

It is well understood that shape and structure of materials have direct influence on the electrochemical properties in respect of cyclability and performance [32]. However, there are yet few works reported to enhance the electrochemical performance with additional doping in $Mn_2O_3$ like materials. The electrochemical performance of all $Al_xMn_{2-x}O_3$ compositions was obtained to determine the Al doping effect. Figs. 4 (b), (c) show the first cycle curves for charging and discharging process of all the samples. A wide sharp plateau can be seen in all first discharge curves at various values. The similar fact was also observed in some previous reports [33]. The obtained initial discharge capacity for Al substituted compositions is higher than that of un-doped $Mn_2O_3$. The lowest charge capacity was observed for $Mn_2O_3$ while highest for composition doped with maximum value of Al. Cycling

performance of all compositions was measured as shown in Fig. 4 (d). Saturation in capacity was reached after a sharp initial decrease. It was found that Al doped compositions show enhanced capacity values after maximum number of cycles. It can be realized that Al substitution in $Mn_2O_3$ improves the electrochemical properties.

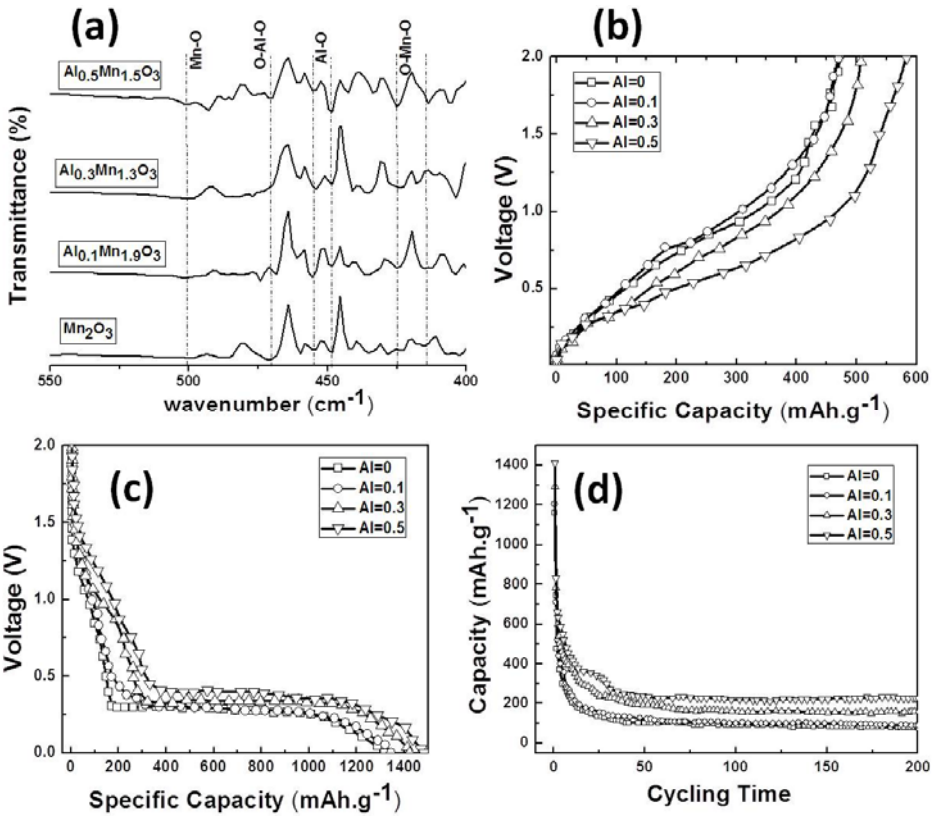


Fig. 4 (a) FTIR spectra and (b-d) electrochemical performance of undoped and Al doped compositions

## IV. Conclusions

Al incorporated $Mn_2O_3$ compositions were successfully synthesized to study the effect of Al doping on electrochemical performance of host material. XRD analysis confirm the phase stability and explore the variation in lattice parameters, crystallite size, lattice strain, density and cell volume. Morphology and elemental composition analysis were in good agreement with the dissolved concentrations of Al in host material. The FTIR results exhibit the O-Al-O and O-Mn-O and Al-O bonding and with increasing the concentration of Al, the vibrational peaks become sharper. An indication of enhanced electrochemical performance in compositions with incorporation of Al content is considerably important for application point of view.

## Acknowledgement

Supported by Deanship of Scientific Research at King Saud University through the research group project No. RG 1435–004.

## References

[1] C. Liu, F. Li, L.P. Ma, H.M. Cheng, Adv. Mater. 22 (2010) E28-E62.
[2] M.S. Whittingham, MRS Bull. 33 (2008) 411-419.
[3] B. Scrosati, J. Hassoun, Y.K. Sun, Energy Environ. Sci. 4 (2011) 3287-3295.
[4] M. Broussely, P. Biensan, B. Simon, Electrochim. Acta. 45 (1999) 3-22.
[5] P. Kristin, A.S. Vijay, H.H. Laurence, H. Yoyo, S.M. Ying, V.V. Anton, S. Venkat, K. Robert, C. Gerbrand, J. Phys. Chem. Lett. 1 (2010) 1176-1180.
[6] H.B. Wu, J.S. Chen, H.H. Hng, X.W. Lou, Nanoscale 4 (2012) 2526-2542.
[7] A.C. Dillon, L.A. Riley, Y.H. Kim, C. Ban, D.T. Gillaspie, A. Pesaran, S.H. Lee, Nanostructured Metal Oxide Anodes, NREL, DOE Merit Review (2009).
[8] A.A. Salvatore, P. Bruce, B. Scrosati, J.M. Tarascon, W.V. Schalkwijk, Nat. Mater. 4 (2005) 366-377.
[9] D. Yang, J. Power Sources 228 (2013) 89-96.
[10] H. Zhimi, X. Xiao, C. Chen, T. Li, L. Huang, C. Zhang, J. Su, L. Miao, J. Jiang, Y. Zhang, J. Zhou, Nano Energy 11 (2015) 226-234.
[11] L.D. Burke, J.F. Healy, J. Electroanal. Chem. 124 (1981) 327-332.
[12] J.E. Arthur, J.M. Meredith, N.R. Philip, T.B. Alexis, T.D. Tilley, J. Phys. Chem. C 113 (2009) 15068-15072.
[13] J.B. Wu, Y. Lin, X.H. Xia, J.Y. Su, Q.Y. Shi, Electrochim. Acta 56 (2011) 7163-7170.
[14] X.H. Huang, J.P. Tu, B. Zhang, C.Q. Zhang, Y. Li, Y.F. Yuan, H.M. Wu, J. Power sources 161 (2006) 541-544.
[15] J.Y. Xiang, J.P. Tu, X.H. Huang, Y.Z. Yang, J. Solid State Electrochem. 12 (2008) 941-945.
[16] F. Li, Y.X. Zhang, M. Huang, Y. Xing, L.L. Zhang, Electrochim. Acta 154 (2015) 329- 337.
[17] Z.K. Ghouri, M.S. Akhtar, A. Zahoor, A.A. Barakat, W. Han, M. Park, B. Pant, P.S. Saud, C.H. Lee, H.Y. Kim, J. Alloys compd 642 (2015) 210-215.
[18] A.A. Salvatore, P. Bruce, B. Scrosati, J.M. Tarascon, W.V. Schalkwijk, Nat. Mater. 4 (2015) 366-377.
[19] N.R. Ravinder, G.R. Ramana, J. Power Sources 124 (2003) 330-337.
[20] J Kuei, W.C. Hseieh, W.T. Tsai, J. Alloys Compd. 461 (2008) 667-674.

[21] M.T. Lee, J.K. Chang, Y.T. Hsieh, W.T. Tsai, J. Power Sources, 185 (2008) 1550-1556.
[22] D.P. Dubal, A.D. Jagadale, S.V. Patil, C.D. Lokhande, MRS Bull. 47 (2012) 1239-1245.
[23] J.M. Luo, B. Gao, X Ghang, MRS Bull. 43 (2008) 1119-1125.
[24] C.S. Ferreria, R.R. Passos, L.A. Pocrifka, J. Power Sources 271 (2014) 104-107.
[25] T.C. Wen, H.M. Kang, Electrochim. Acta 43 (1998) 1729-1745.
[26] D.L. Fang, Z.D. Chen, B.C. Wu, Y. Yan, C.H. Zheng, Mater. Chem. Phys. 128 (2011) 311- 316.
[27] G. Adylov, V. Voronov, L. Sigalov, Inorg. Mater. 23 (1988) 1867-1870.
[28] R.V. Sagar, S. Buddhudu, Spectrochim. Acta A 75 (2010) 1218-1222.
[29] N. Varghese, M. Hariharan, D.A.B. Cherian, D.P.V. Sreenivasan, J. Paul, A.K.A. Antony, Int. J. Sci. Res. Pub. 4 (2014) 2250-3153.
[30] K. Lipping, M. Zhang, Z.H. Liu, K. Ooi, Spectrochim. Acta A 67 (2007) 864-869.
[31] S.A. Hosseini, A. Niaei, D. Salari, Open J. Phys. Chem. 1 (2011) 23-27.
[32] R. Ma, M. Wang, P. Tao, Y. Wang, C. Cao, G. Shan, S. Yang, L. Xi, J.C.Y. Chung, Z. Lu, J. Mate. Chem. A 1 (2013) 15060-15067.
[33] L. Hu, Y. Sun, F. Zhang, Q Chen, J. Alloys Compd. 576 (2013) 86-92.